J. Membrane Biol. 183, 51–60 (2001)
DOI: 10.1007/s00232-001-0052-y

The Journal of
Membrane
Biology

External Nickel Blocks Human Kv1.5 Channels Stably Expressed in CHO Cells

L. Perchenet, O. Clément-Chomienne
Preclinical Research, Department of Vascular and Metabolic Diseases, F. Hoffmann-La-Roche Ltd., PRBM, Bau 70/423, Grenzacherstr. 124, CH-4070 Basel, Switzerland

Received: 12 October 2000/Revised: 14 May 2001

Abstract. We have investigated the actions of Nickel (Ni^{2+}) on a human cardiac potassium channel (hKv1.5), the main component of human atrial ultra-rapid delayed rectifier current, stably expressed in Chinese hamster ovary cell line using the whole-cell voltage-clamp technique. External Ni^{2+} reversibly decreased the amplitude of the current in a concentration-dependent manner. The concentration for half-maximum inhibition of the current at +50 mV was 568 μM. The activation, deactivation, reactivation kinetics of the current were not affected by Ni^{2+}. Block was not voltage-dependent but frequency-dependent block was apparent. The extent of channel block during the first pulse increased when the duration of exposure to Ni^{2+}, prior to channel activation, was prolonged indicating that Ni^{2+} interacted with hKv1.5 in the closed state. The percentage of current remaining in presence of Ni^{2+} decreased steeply over the range of steady-state channel inactivation, consistent with an enhanced block with increased inactivation. This suggests that Ni^{2+} preferentially blocks nonconducting hKv1.5 channels, either in the resting or inactivated state in a concentration-dependent manner. The data indicate that the mechanisms of hKv1.5 channel inhibition by Ni^{2+} are distinct from those of other K^+ channels.

Key words: K^+ channels — hKv1.5 — Ultra-rapid delayed rectifier K^+ current — Nickel — Channel blockade

Introduction

In the myocardium, K^+ currents carried through a number of distinct voltage-dependent K^+ channels play an important role in cardiac repolarization. Molecular biological studies have led to the cloning of a variety of genes, expressed in mammalian heart, which encode proteins that underlie some of the repolarizing voltage-dependent potassium channels. These include several members of the family of Shaker-related voltage-gated K^+ channels, pore-forming alpha subunits discovered in cardiac tissue (Barry et al., 1995; Roberds et al., 1993). One of which, Kv1.5 (hKv1.5), is thought to underlie the 4-aminopyridine-sensitive ultra-rapidly activating delayed rectifier K^+ current (I_{Kur}) found in human atrial myocytes. Studies with antisense oligonucleotides provided direct evidence that hKv1.5 is essential to the functional expression of the human atrial I_{Kur} (Feng et al., 1997). Kv1.5 transcript (Fedida et al., 1993) and hKv1.5 protein (Mays et al., 1995) have also been detected in human ventricle despite the absence of corresponding current (Li et al., 1996). It is possible that the hKv1.5 alpha-protein contributes to the K^+ current in the ventricle through the formation of heteromultimeric K^+ channels with other Shaker-like alpha-subunits (Mays et al., 1995).

The pharmacology of hKv1.5 has been studied quite extensively and several structurally distinct compounds have been shown to nonspecifically block currents due to the expression of human hKv1.5 homomultimers. Local anesthetics like bupivacaine, ropivacaine, mepivacaine have been shown to block hKv1.5 (Franqueza et al., 1998; Longobardo et al., 1998), as were a fungicide (ketoconazole) (Dumaine, Roy & Brown, 1998) and nonsedating histamine antagonist (Delpon et al., 1997; Yang et al., 1995). Class I and III antiarrhythmic agents, used to maintain sinus rhythm and for the treatment of ventricular tachycardia, are known to block hKv1.5 in the therapeutical range (Franqueza et al., 1998; Malayev, Nelson & Philipson, 1995).

Divalent and trivalent metal ions, and in particular Ni^{2+}, are well-established blockers of various subtypes of voltage-dependent calcium channels and cardiac K^+

Correspondence to: O. Clément-Chomienne
odile.chomienne@roche.com

channels. Ni^{2+} is thought to preferentially block the T-type calcium channel (for review, *see* Hille, 1992) and has been employed as a tool to discriminate T-type currents from other calcium current types; however, there are a number of non-T-type calcium currents which are highly sensitive to Ni^{2+}, and at sufficiently high concentration, Ni^{2+} blocks all the cloned and transiently expressed calcium channels (Zamponi, Bourinet & Snutch, 1996). Recent studies have revealed that the voltage-gated cloned channel encoded by HERG (human ether-a-go-go related gene) is nonselectively blocked by most divalent cations (including Ni^{2+}, Co^{2+} and Ba^{2+}) from the external side (Ho et al., 1999). These divalent cations decrease the amplitude of the cardiac rapid component of the delayed rectifier K^+ current (I_{Kr}) (Song, Earm & Ho, 1999) and Shi, Wang & Wang, (2000) have demonstrated that Ba^{2+}, in addition to its well-known effects on the inward rectifier K^+ current, produced significant inhibition of the transient outward K^+ channel (I_{to}). However, there is very little information available concerning the action of divalent cations on I_{Kur} or shaker-type voltage-gated K^+ channels (Wang, Fermini & Nattel, 1993). The present study was undertaken to characterize the concentration-, voltage-, and state-dependent blockade by Ni^{2+} of hKv1.5 channels expressed in a stable mammalian Chinese hamster ovary (CHO) cell line.

Materials and Methods

Cell Preparation

Effect of Ni^{2+} has been determined using a stable mammalian cell line stably expressing human Kv1.5 voltage-gated potassium current (Tamkun et al., 1991). Endogenous voltage-gated potassium channels are expressed in human embryonic kidney (HEK 293) cells (Yu & Kerchner, 1998). Since no appreciable endogenous currents were detected in nontransfected Chinese hamster ovary cell line (Philipson et al., 1993), we chose a CHO cell line as an expression system to study hKv1.5. The CHO cells were maintained at 37°C in Minimum Essential Eagle's Medium Alpha (Gibco/BRL, Basel, Switzerland) supplemented with 10% fetal bovine serum (Gibco/BRL) and 1% penicillin-streptomycin (Gibco/BRL) under a 5% CO_2 atmosphere. Cells were plated on Poly-D-lysin (PDL)-treated culture dishes (Sigma, Buchs, Switzerland) every 2–3 days after brief treatment with trypsin-EDTA (Gibco/BRL). For electrical recordings, cells were trypsinized and seeded on acid-washed and PDL-coated coverslips and used within 48 hours. Nontransfected CHO cells did not display any voltage- or time-dependent outward current (*see* Fig. 1*A*).

Electrical Recording

CHO cells on coverslips were placed in a perfused recording chamber RCP-10T (Dagan, Minneapolis, MN, USA) on the stage of an inverted microscope (Eclipse, Nikon, Basel, Switzerland). Bath solution flowing out of a quartz micromanifold (ALA Scientific Instruments, NY, USA) was directed onto individual cells to quickly apply various external drug-containing solutions. Outward potassium currents were measured at room temperature (18–19°C) using the whole-cell configuration of the patch-clamp technique (Hamill et al., 1981). Pipettes were prepared from borosilicate capillary glass (Hilgenberg, Malsfeld, Germany) with a Sutter P-97 puller (Sutter Instrument, Novato, NY) and CPM-2 ALA microforge (ALA Scientific Instruments, New York, NY, USA). Resistances of the patch pipettes were between 2 and 3 MΩ. Recordings were performed using an EPC-9 double-patch-clamp amplifier (HEKA Elektronik, Lambrecht/Pfalz, Germany). Pipette potential and capacitance were nulled and a 5–15 GΩ seal formed with the cell membrane. Voltage-clamp protocols were applied using Pulse software (Heka Elektronik) and whole-cell current recordings were displayed and analyzed using Pulse and Pulsefit software (Heka Elektronik). Except when specified, the amplitude of the hKv1.5 current expressed in CHO cell line was assessed at the end of 250 msec command pulse voltages applied every 15 sec between −70 and +70 mV from a holding potential of −70 mV. Deactivation of tail current was recorded upon repolarization to −40 mV. Tail-current amplitude was calculated as the difference between the peak amplitude of the tail and the sustained level of current after 200 msec of repolarization to −40 mV. Membrane potentials were corrected for a liquid junction potential between the pipette and the bath solutions and whole-cell capacitance and series resistance (*Rs*) compensations were optimized to minimize capacitive currents and reduce voltage errors. Macroscopic current values were normalized for cell capacitance and expressed in picoamps per picofarad. All values are presented as mean ± SEM. 56 CHO cells were clamped and the average cell capacitance obtained was 18.2 ± 1.1 pF.

The standard bath solution employed in the experiments contained the following (mM): 140 NaCl, 5 KCl, 1 $MgCl_2$, 2 $CaCl_2$, 10 HEPES, 5 glucose, pH was adjusted to 7.3. The whole-cell pipette solution contained the following (mM): 130 KCl, 1 $MgCl_2$, 10 HEPES, 5 BAPTA, 3 Na_2ATP, 5 glucose, pH adjusted to 7.2. Na_2ATP and BAPTA were obtained from Sigma.

Statistical Method

All values in the text and in figures are presented as means ± SEM. Direct comparisons between mean values in control conditions and in the presence of Ni^{2+} for a single variable were performed by paired Student's *t*-test. A level of $P < 0.05$ was considered to be statistically significant.

Results

Concentration-Dependent and Reversible Block of hKv1.5 by Ni^{2+}

Figure 1 shows the effects of Ni^{2+} on macroscopic hKv1.5 current of successfully transfected CHO cells recorded in the whole-cell configuration. A record from a control, nontransfected cell is also shown for comparison, demonstrating the lack of voltage-gated current in absence of transfection (Fig. 1*A* top). Figure 1*A* bottom shows superimposed hKv1.5 outward potassium current recordings from a transfected CHO cell in control conditions and in the presence of increasing concentrations of Ni^{2+}. hKv1.5 currents were induced by a 250 msec clamp pulse to +50 mV from a holding potential of −70 mV every 15 sec. Under control conditions, the outward

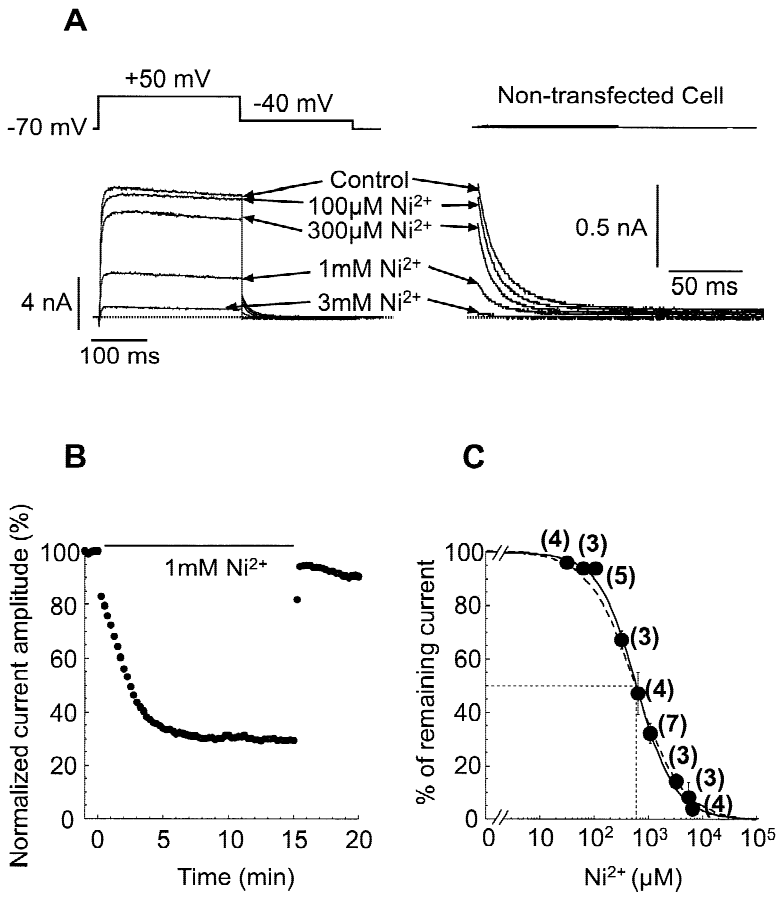

Fig. 1. Inhibition by Ni^{2+} of hKv1.5 expressed in mammalian CHO cell line. (*A*) Concentration-dependent inhibition by Ni^{2+} of hKv1.5 current elicited by a 250 msec pulse applied from −70 mV to +50 mV and corresponding tail current obtained during repolarization at −40 mV. Nontransfected cell did not display any current. (*B*) Time course of current inhibition by 1 mM Ni^{2+} and reversibility. (*C*) Dose-response relationship for Ni^{2+} block. Data obtained from 3 to 7 cells, using the same protocol as shown in (*A*) were averaged and plotted against Ni^{2+} concentration. A nonlinear least-squares equation fitted the data points with a free Hill coefficient (continuous line) and with a Hill coefficient fixed to 1 (dashed line).

current rose rapidly to a peak and then partially inactivated with a slow time course. Slowly decaying outward tail currents were recorded upon repolarization to −40 mV. Ni^{2+} produced a concentration-dependent decrease in both net outward and tail current amplitude. After a tonic block of 16 ± 1% ($n = 7$) was achieved during the first pulse in the presence of 1 mM Ni^{2+}, subsequent pulses delivered at a frequency of 0.066 Hz induced a slow progressive decline in the amplitude of net outward current up to 32 ± 3% ($n = 7$) of the initial level of current. Moreover, 1 mM Ni^{2+} reduced the peak outward current by 61 ± 4% ($n = 7$) compared to control and did not alter the time course of the current during depolarization, so that the reduction of the current at the end of the 250 msec depolarizing pulse was 68 ± 4% ($n = 7$) compared to control. The effect of Ni^{2+} was complete and stable after a period of 5–7 min and was rapidly reversed upon washout of the cation by superfusion with control solution (Fig. 1*B*). The time course of the Ni^{2+} effect was not contaminated by the time course of solution exchange in the bath, since the solutions were applied directly to the cells using a quartz micromanifold. Figure 1*C* shows the concentration dependence of Ni^{2+} block of hKv1.5 over a range of concentration between 30 μM and 6 mM. A nonlinear least-squares fit of the concentration-response equation to the individual data points yielded an apparent affinity constant (K_D) of 568 ± 24 μM and a Hill coefficient of 1.23 ± 0.06. When the data were fitted with the Hill coefficient constrained to 1, a similar value for the apparent affinity constant was obtained ($K_D = 567 \pm 48$ μM). These results suggest that binding of one Ni^{2+} ion per channel is sufficient to block potassium permeation.

Voltage-independent Block of Kv1.5 by Ni^{2+}

Figure 2*A* shows representative families of hKv1.5 currents evoked by a series of 250 msec test pulses between −70 and +70 mV from a holding potential of −70 mV before and in the presence of 1 mM Ni^{2+}. Average current-voltage relations for net whole-cell and tail current density in control conditions or in the presence of 1 mM Ni^{2+} ($n = 7$) are shown in Fig. 2*B*. The net *I-V* relationship was linear for depolarizations positive to −30 mV. Ni^{2+} significantly reduced the amplitude of hKv1.5 at all voltages positive to −30 mV, as is evident from the change in net and tail currents in the families of whole-cell current. Due to differences in expression, the amplitude of hKv1.5 current differed considerably between

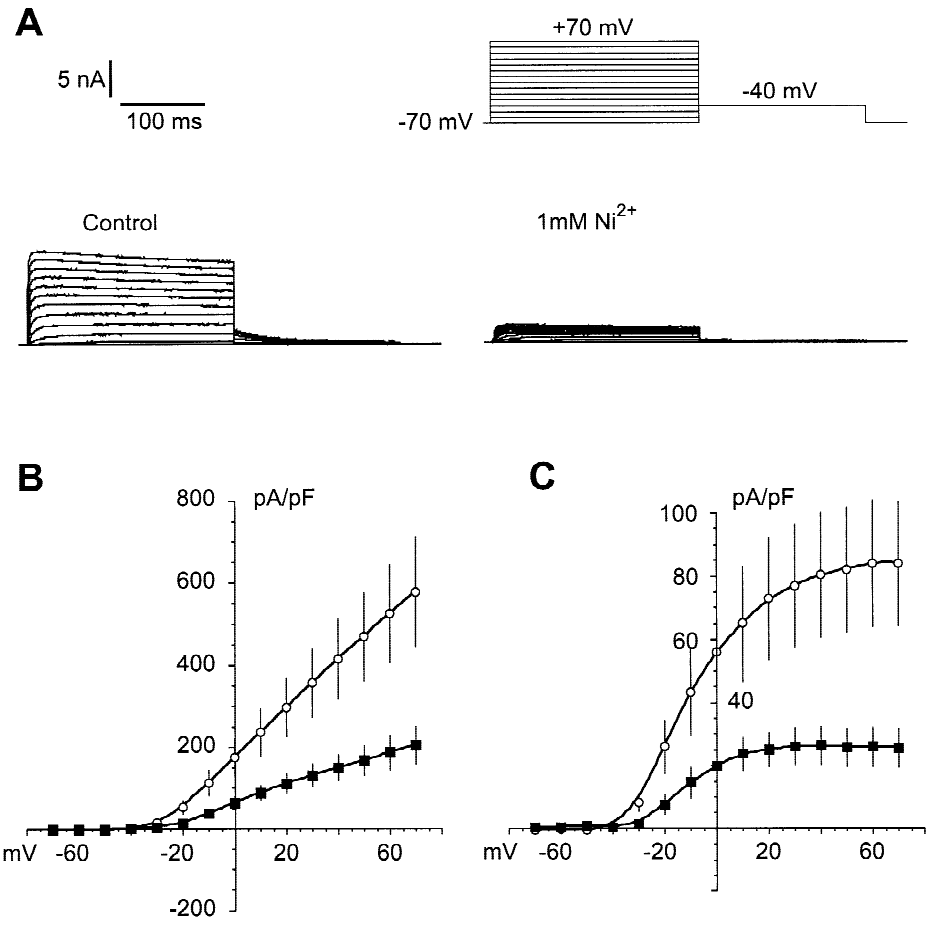

Fig. 2. Effect of external Ni^{2+} on hKv1.5 elicited by depolarizing voltage pulses. (*A*) Representative families of current traces elicited by depolarizing voltage pulses of 250 msec in 10 mV steps from a holding potential of −70 mV in control conditions and in the presence of 1 mM Ni^{2+}. (*B*) Plot of the current density measured at the end of depolarizing pulses *versus* the pulse potential in control (○) and in the presence of 1 mM Ni^{2+} (■; $n = 7$ cells). (*C*) Average current-voltage relationship for tail currents obtained in control (○) conditions and in the presence of 1 mM Ni^{2+} (■; $n = 7$ cells).

CHO cells and therefore average net and tail currents recorded from 7 cells had relatively large SEM values. To determine and quantify the voltage-dependence of this inhibition, the percentage of current inhibition by Ni^{2+} was plotted as a function of voltage (Fig. 3) for command steps of 250 msec and 10 sec in duration. Between −20 and +70 mV, the level of block induced by Ni^{2+} was constant for both durations of pulses and there was no evidence of any voltage-dependence of inhibition by Ni^{2+}.

Lack of Effect of Ni^{2+} on Kinetics of Activation, Deactivation and Recovery of hKv1.5

Activation and deactivation kinetics for the time-dependent current during the 250 msec command pulses between −10 and +70 mV and tail currents at −40 mV were determined: both activation and deactivation of hKv1.5 were best fit with a bi-exponential function over the entire range of incremental steps of depolarization. Between −10 and +70 mV no significant difference was found for the slow (Fig. 4*A*) and fast (Fig. 4*B*) time constant of activation before and after treatment with Ni^{2+}. At +50 mV, the values of the fast activation time constant were, respectively, 0.74 ± 0.26 msec and 0.86 ± 0.35 msec in control conditions and in the presence of 1 mM Ni^{2+}. Slow time constants were 5.75 ± 3.17 msec and 4.46 ± 1.11 msec before and after Ni^{2+} treatment, respectively. Similarly, deactivation fast and slow time constants were not affected by the Ni^{2+} block. During repolarization at −40 mV after a test pulse at +50 mV, the value of fast deactivation time constant was 20.90 ± 2.75 msec and 18.10 ± 4.53 msec in control conditions and in the presence of 1 mM Ni^{2+}, respectively. Slow time constants were 67.10 ± 7.02 msec and 65.5 ± 6.70 msec

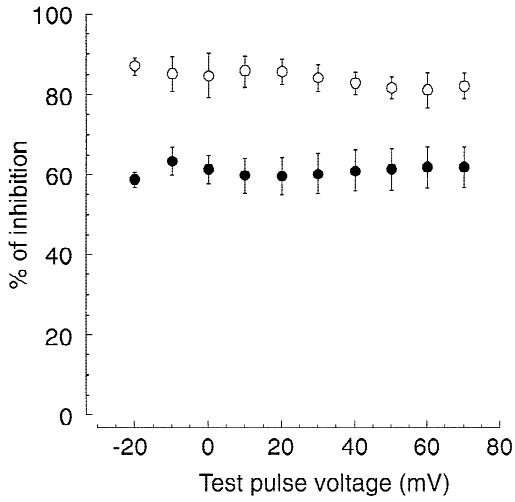

Fig. 3. Absence of voltage-dependence of Ni^{2+} inhibition. Average percentage of inhibition of hKv1.5 by 1 mM Ni^{2+}, measured at the end of a 250 msec (●; $n = 7$ cells) or a 10 sec (○; $n = 5$ cells) test pulse, is plotted *versus* the test-voltage amplitude. No significant voltage-dependence was observed for the block induced by Ni^{2+}.

before and after Ni^{2+} treatment, respectively. The lack of any change in deactivation kinetics and the absence of a "crossover" phenomenon (Fig. 1*A*) might indicate that unblock was not necessary for channel closure or that the rate of channel unblocking might be too slow to produce significant current during the tail recording.

Recovery from inactivation was studied using a double-pulse protocol: whole-cell current was inactivated by a 4 sec prepulse to +40 mV and the extent of recovery from inactivation determined by applying a second 0.7 sec pulse to the same voltage after a variable time between 0.4 and 60 sec, at −70 mV. The very slow inactivation kinetics of hKv1.5 precluded measurements of recovery from a true condition of steady-state inactivation. The average percentage ($n = 6$) of recovery between the prepulse and each second pulse was plotted against the interpulse interval duration in Fig. 5. In both conditions, the data were best fitted with a bi-exponential function yielding recovery time constants that were not significantly different in the presence of Ni^{2+} (1.05 ± 0.16 sec and 17.34 ± 1.21 sec in control *versus* 1.03 ± 0.11 sec and 16.06 ± 0.42 sec with 1 mM Ni^{2+}).

Effect of Ni^{2+} on Activation and Inactivation Voltage-Dependence

To assess the effect of Ni^{2+} on the voltage-dependence of activation and inactivation of hKv1.5, steady-state availability and activation curves were determined for traces obtained in the absence and in the presence of 1 mM Ni^{2+} in 5 cells. To determine the effect of Ni^{2+} on the voltage-dependence of activation, the amplitude of tail currents recorded at −40 mV following depolarizing steps between −70 and +70 mV were normalized to maximum tail-current amplitude and plotted against command-step potential (Fig. 6*A* and *C*). The data for both conditions were best fitted with a single Boltzmann function. The voltage-dependence of activation for the two data sets was identical, as illustrated by a lack of significant difference in the values for the half-activation ($V_{0.5}$) and slope factor (k) of the Boltzmann functions (Fig. 6). The value for the mid-point of activation in control conditions obtained in this study is consistent with that previously reported for hKv1.5 expressed in CHO cells (Philipson et al., 1993).

Figure 6*C* shows the steady-state availability of hKv1.5 determined using a standard double-pulse protocol. As described in panel *B*, ten second prepulses to potentials between −80 and +30 mV in 10 mV intervals were applied every 45 sec to inactivate the channels. Each prepulse was followed by a brief 5 msec hyperpolarizing step to −130 mV and a 200 msec test pulse to a constant voltage of +30 mV. Average values for peak outward current during the test pulse were normalized to the maximal amplitude and plotted against the voltage of the prepulse step. Due to the slow inactivation kinetics of hKv1.5 it was impossible to achieve a true steady-state condition for the whole-cell current, but the duration of the 10 sec prepulse step was sufficient for the current to decline to a relatively stable level. Both sets of data were best fitted with single Boltzmann functions yielding values for half maximal of availability of −24.6 ± 0.9 mV and −24.5 ± 0.5 mV before and during Ni^{2+} treatment, respectively, that were not different. The value in control conditions was consistent with that previously reported for hKv1.5 expressed in CHO cells (Philipson et al., 1993). However, in the presence of Ni^{2+}, the level of residual, non-inactivating current was significantly lower (21 ± 7%, $n = 5$) compared with the level obtained in control conditions (47 ± 4%, $n = 5$). This suggested to us the possibility that Ni^{2+} may interact with the inactivated state of hKv1.5.

Frequency-Dependence of Block

The mechanism of channel block by Ni^{2+} was examined first by assessing the effect of changes in stimulation frequency on the inhibition of hKv1.5 current (Fig. 7*A* and 7*B*). Depolarizing pulses from −70 mV to +40 mV were applied at three different stimulation frequencies, 0.02, 0.2 and 2 Hz in the absence (control) and presence of 1 mM Ni^{2+}. Under control conditions, the current amplitude remained constant during the repetitive application of pulses during a train of 15 pulses at 0.02 Hz. At 0.2 Hz and 2 Hz, the control outward current declined

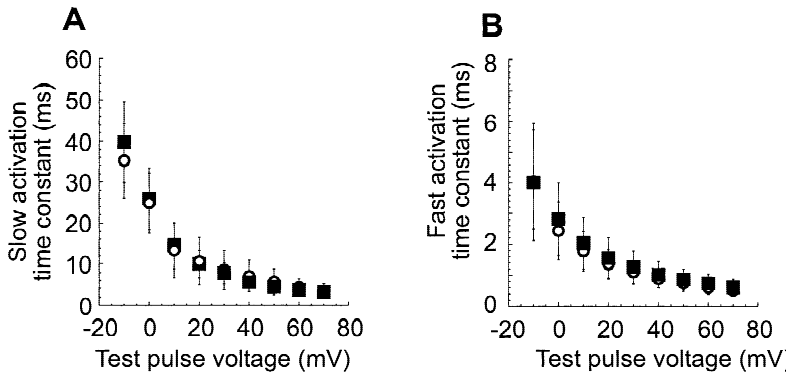

Fig. 4. Effect of 1 mM Ni^{2+} on the kinetics properties of hKv1.5 current. Current activation was fitted with a double exponential function, and the slow (*A*) and fast (*B*) time constants were plotted against test potential. Mean ± SEM obtained from 7 cells are represented in control conditions (○) and in the presence of Ni^{2+} (■).

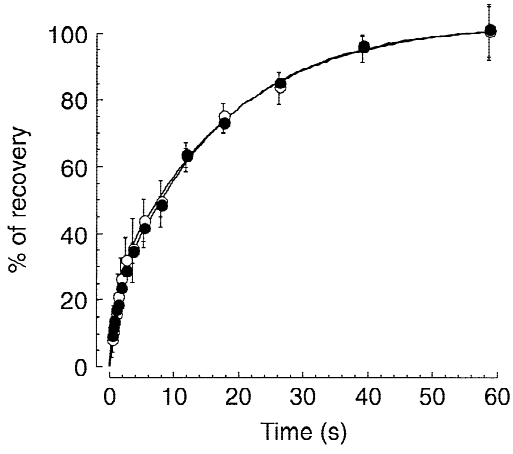

Fig. 5. Recovery from inactivation. Whole-cell current was inactivated by a 4 sec prepulse to +40 mV and the extent of recovery from inactivation determined by applying a second 0.7 sec pulse to the same voltage after a variable interval at −70 mV between 0.4 and 60 sec. Fractional recovery from inactivation was plotted as a function of interpulse duration for hKv1.5 in control conditions (○) and in the presence of 1 mM Ni^{2+} (●). The continuous lines represent double-exponential functions that were the best fit to the data points ($n = 6$ cells).

by 5 and 25%, respectively, likely due to insufficient time for complete recovery of inactivation between two pulses (Feng et al., 1998). At all frequencies of stimulation, there was an apparent frequency-dependent block due to Ni^{2+} (Fig. 7*A*). The amplitude of current progressively decreased until a new steady-state level was reached. This additional block was completed after a train of 20 pulses at 0.2 Hz and 40 pulses at 2 Hz. To describe the apparent use-dependent effect of the divalent cation without complications of the decline of the current under control conditions, Fig. 7*B* represents the relative current ($I_{Ni}/I_{control}$) elicited during the application of these pulse protocols as a function of the number of pulses. As it is shown, the degree of hKv1.5 block was significantly increased with the driven rate.

Mechanism of Channel Block

A lack of open-state channel block by Ni^{2+} was indicated by: i) the absence of an increased rate of decay in current amplitude during short, 250 msec test pulses, and ii) a lack of voltage-dependence of the block, even for very long depolarizing steps, which would be expected to permit a slowly developing open channel block. If Ni^{2+}-binding was primarily to the open state, the block would have been expected to increase steeply over the voltage range of channel activation. These data suggested to us that the block of hKv1.5 by Ni^{2+} occurred in a nonconducting state, i.e. the resting and/or inactivated state.

As shown in Fig. 1, Ni^{2+} produced an immediate 16 ± 1% block of hKv1.5 end pulse current after only 15 sec of rest at −70 mV and thereafter, it declined slowly to a maximum after about 5 min. If Ni^{2+} interacted with the channel in the closed state, it would be expected that the initial level of current suppression would be greater if the time before the first command pulse after exposure to Ni^{2+} was increased. To determine if this occurred, the first pulse was delayed for 0.5, 2 and 5 min. Figure 7*C* shows that the initial percentage of tonic block was indeed greater when the interval of time between application of Ni^{2+} and the first 250 msec command pulse was increased. At 2 and 5 min, the level of block increased to approximately 62 and 68%, respectively, accounting for most of the reduction in current amplitude and equivalent to the maximum level of current inhibition attained after 5 min of continuous pulsing (approximately 68%). Additional experiments were conducted employing a very negative holding potential of −110 mV to control for occasional transitions to the open state at −70 mV (*data not shown*). No difference in the extent of block by Ni^{2+} was apparent and a stable level of block was attained after 5 min. These data support the view that Ni^{2+} interacts with the closed state of hKv1.5 channels.

The decrease in residual, non-inactivating hKv1.5 current in the presence of Ni^{2+} (Fig. 6) suggested the possibility that the cation may have interacted with the channels while in the inactivated state. To assess wheth-

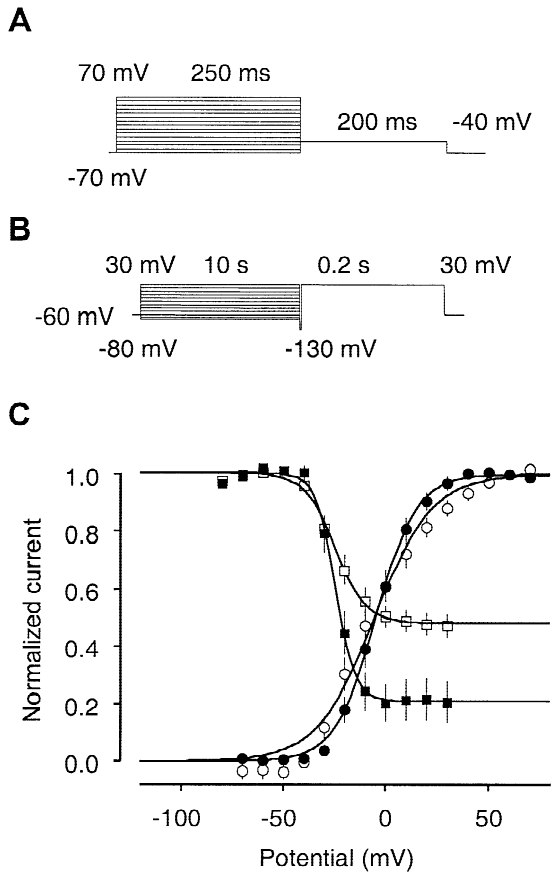

Fig. 6. Voltage-independence of hKv1.5 block. (*A*) Voltage protocol used to produce activation relationships. (*B*) Voltage protocol used to evaluate steady-state availability. (*C*) Activation curves were drawn by fitting the normalized tail-current amplitude to the Boltzmann equation $Y_\infty = \{1 + \exp[(V_{0.5} - V)/k]\}^{-1}$. Data are mean ± SEM from 5 cells. $V_{0.5}$ and slope factor (k) are −12.2 ± 0.7 and 10.6 ± 0.6 mV in control conditions (○) and −13.5 ± 0.5 and 7.8 ± 0.5 mV in the presence of Ni^{2+} (●). Steady-state availability relations for hKv1.5 channels were obtained by plotting normalized current amplitude during test pulse at +30 mV *versus* the voltage of a 10 sec prepulse. The data points were fitted with the Boltzmann equation $Y_\infty = \{1 + \exp[(V - V_{0.5})/k]\}^{-1}$. Data represent mean ± SEM from 5 cells. $V_{0.5}$ and slope factor (k) were −24.6 ± 0.9 and 7.63 ± 0.8 mV in control conditions (□) and −24.5 ± 0.5 and 4.9 ± 0.4 mV in the presence of Ni^{2+} (■).

er channel inactivation facilitated block by Ni^{2+}, cells were held at different potentials between −70 and +40 mV in control conditions and after application of Ni^{2+}. The fractional current remaining at the end of 200 msec depolarizing pulses in the presence of 1 mM Ni^{2+} was plotted as a function of the holding potential (Fig. 8*A*). According to the voltage-dependence of the inactivation curve displayed in Fig. 6, the current began to inactivate at −40 mV and the channel was fully inactivated at +10 mV. Figure 8*A* shows that the percentage of remaining current decreased steeply over the range of steady-state channel inactivation between −40 and +10 mV, consistent with an enhanced block with increased inactivation. In Fig. 3, the percentage of block induced by 1 mM Ni^{2+} was larger for long-duration protocols compared with short-duration protocols at all voltages tested. This suggested that the fraction of block obtained in the closed state could be increased by inactivation of the channel. To directly assess whether this was the case, we applied depolarizing steps of increasing duration after stable block was already obtained in the closed state with 250 msec duration pulses in the presence of 1 mM Ni^{2+} (n = 3). Sequentially increasing the number of inactivated channels by applying depolarizing steps of greater duration increased the extent of block during subsequent pulses beyond the level achieved in the absence of inactivation. This effect could not be an artifact of partial recovery from the inactivated state (Feng et al., 1998), since the same long-duration depolarizing protocol tested in control conditions did not result in a subsequent decrease in peak current (*see* inset Fig. 8*B*).

Discussion

In the present study we have analyzed the effect of Ni^{2+} on the cardiac human Kv1.5 stably expressed in a mammalian cell line. We have shown for the first time that Ni^{2+} blocks hKv1.5 channels in a concentration-dependent and reversible fashion. Ni^{2+} did not affect the kinetics of activation, deactivation, or recovery from inactivation of hKv1.5, nor did it modify the voltage-dependence of activation or inactivation. There was no evidence of voltage-dependence of block by Ni^{2+}, suggesting a lack of inhibition in the open state. However, the extent of block by Ni^{2+} was increased by the duration of exposure prior to channel activation and by the extent of current inactivation during long depolarizing pulses consistent with an interaction with nonconducting, resting and/or inactivated states. These results suggest that the state-dependence of hKv1.5 channel block by Ni^{2+} is different from that previously reported for other voltage-gated K^+ channels, such as HERG and I_{Kr}, which are blocked by divalent cations in the activated state (Ho et al., 1999; Song et al., 1999).

The interaction of Ni^{2+} with hKv1.5 channels was voltage-independent between −20 and +70 mV, even for long-duration 10 sec pulses. An increased extent of channel block at more positive test pulses was not observed. Moreover, Ni^{2+} did not accelerate the rate of hKv1.5 current decay during 250 msec step depolarizations and we did not observe the development of a bi-exponential time course of current decay in the presence of Ni^{2+} even for 10 sec step depolarizations. These results are all inconsistent with an open-channel block mechanism, since an increase in block would be expected as the probability of transition to the open state increases with the level of depolarization and duration of depolarization during the command pulses. This conclu-

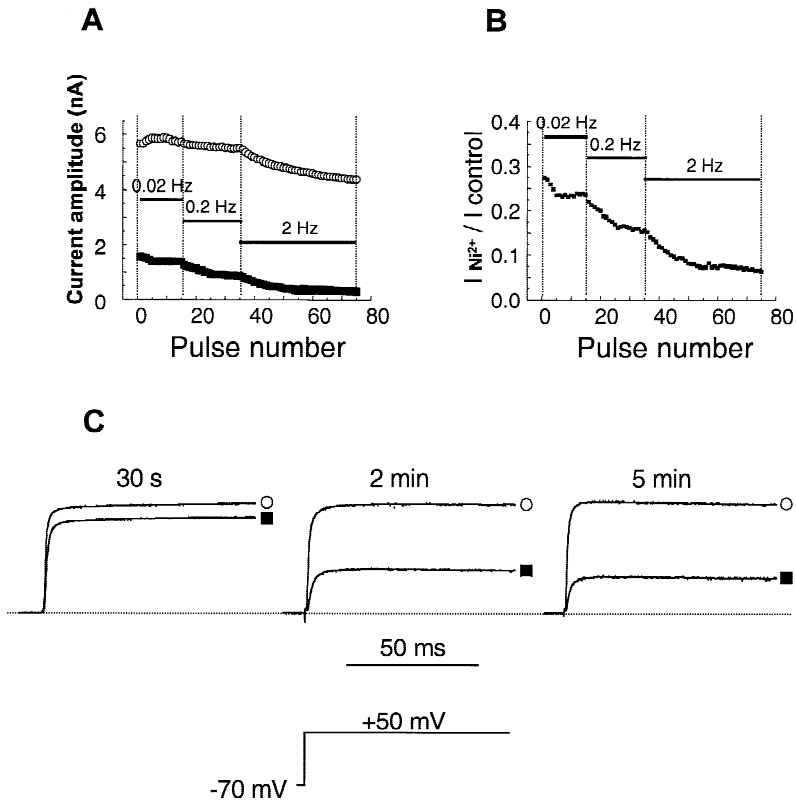

Fig. 7. Frequency-dependence and closed-channel block of hKv1.5. (*A*) Typical data from one cell showing the outward current amplitude measured at 0.02, 0.2 and 2 Hz in control conditions (○) and in the presence of 1 mM Ni^{2+} (■) and expressed as the number of pulses. (*B*) Relative current ($I_{Ni^{2+}}/I_{control}$) at 0.02, 0.2 and 2 Hz was plotted as a function of the number of pulses. (*C*) Original records obtained from three different cells in the absence (○) and in the presence (■) of 1 mM Ni^{2+} when increasing the time between the application of Ni^{2+} and the first depolarizing test in the presence of Ni^{2+}.

sion is also supported by the tail-current data showing that Ni^{2+} did not slow deactivation of hKv1.5 current and did not induce any crossover of the tails.

In all our experiments, hKv1.5 current was significantly reduced during the first pulse in the presence of Ni^{2+} indicating block by the cation-preceded channel activation. Moreover, the extent of channel block during the first pulse increased when the duration of exposure to Ni^{2+} prior to channel activation, was increased. After 5 min, the extent of block was the same regardless of pulsing or keeping the cell at negative holding potential. These data all indicate that Ni^{2+} interacts with hKv1.5 in the closed state. Moreover, relief of Ni^{2+} block upon washout of the cation was almost immediate and did not require channel activation. These data are also consistent with closed-channel block and imply that Ni^{2+} interacts with an external binding site on the channel. The slow onset but rapid relief of Ni^{2+} during washout indicates very disparate rates for Ni^{2+}-association and -dissociation with closed hKv1.5 channels.

The present results also indicate that an interaction between Ni^{2+} and hKv1.5 channels may also occur when they are in the inactivated state. This view is supported by the fact that the extent of channel block was further increased during long-duration pulses to inactivate hKv1.5 channels via a slow, C-type mechanism subsequent to achieving a maximum, stable level in the closed state. Moreover, the extent of block increased with the level of current inactivation during a standard double-pulse protocol to assess the voltage-dependence of hKv1.5 availability. This suggests that Ni^{2+} interacts with greater potency following C-type inactivation of Kv1.5 channel. This mechanism of interaction can explain the apparent frequency-dependence of Ni^{2+} block. Indeed, recovery of inactivation decreases with increasing frequency and the level of block in the inactivated state should increase.

The inhibition of whole-cell hKv1.5 currents by Ni^{2+} described in this study is likely not related to a change in membrane surface charge in the presence of the divalent cation. Varying Ca^{2+} concentration is well known to affect surface charge and the activation of ion channels, including voltage-gated K^+ channels (Hille, 1992). However, even in the presence of 1 mM Ni^{2+}, the voltage-dependence of activation and inactivation of hKv1.5 were unaffected. If the membrane surface charge were important for the effect of Ni^{2+}, we would have expected to observe a shift in the voltage-dependence of activation and inactivation.

The inhibition of hKv1.5 by Ni^{2+} observed in this study appears to be different from that reported for other voltage-gated K^+ channels. For example, the potency of Ni^{2+} block of hKv1.5 channels is comparable to that reported for inhibition of HERG channels expressed in

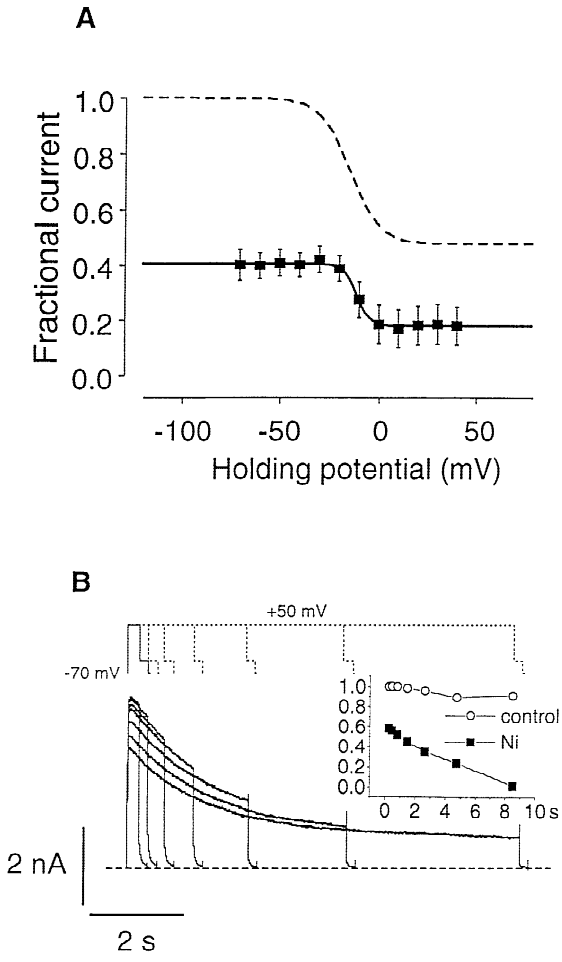

Fig. 8. Ni^{2+} blocks hKv1.5 channel in the inactivated state. (*A*) Fractional hKv1.5 current as a function of the holding potential. The remaining current at the end of a 200 msec depolarizing pulse, in the presence of 1 mM Ni^{2+}, was plotted as a function of the holding potential (solid line; $n = 5$ cells). The dotted line represents the inactivation curve obtained earlier in control conditions. (*B*) Short duration (250 msec) depolarization steps to +50 mV in the presence of 1 mM Ni^{2+} were followed by increasing long-duration pulses (30 sec interpulse interval) after the steady-state of block was obtained. Even after steady state for closed-channel block was reached, Ni^{2+} was able to block the current in its inactivated state. Inset represents the fractional current in control and in Ni^{2+} conditions as a function of pulse duration.

Xenopus laevis oocytes (Ho et al., 1999), but the mechanism of block seems to be different. Ni^{2+} and other divalent cations, such as Ba^{2+}, block HERG in a voltage-dependent manner and affect the kinetics of activation and deactivation, consistent with block in the open state. Ni^{2+} block of hKv1.5 is 4 times more potent than its effect on I_{Kr} from rabbit sinoatrial node cells (Song et al., 1999). I_{Kr} channels are nonselectively blocked by Ni^{2+} and other divalent cations from the external side and due to an interaction with a binding site located deep within the pore, the block demonstrates a steep voltage-dependence. In contrast, Ni^{2+} did not block I_{Kr} of rabbit ventricular myocytes, rather it relieved the extent of inward rectification of the channel (Paquette et al., 1998). Among the voltage-gated K^+ channels thought to be expressed in cardiac muscle, it appears that hKv1.5 has a unique mechanism of block by Ni^{2+}. Indeed, hKv1.5 channels are alone in their interaction with Ni^{2+} in the nonconducting state.

In this study, the effects of Ni^{2+} on hKv1.5 channels were assessed in a mammalian cell line. It is postulated that the hKv1.5 alpha-subunit underlies the ultra-rapid component of the delayed rectifier K^+ current of human atrial myocytes (Feng et al., 1997). Additional studies to evaluate the effect of Ni^{2+} on the native current are warranted to show identity in the mechanism of block of the cloned and native channel currents. Moreover, it would also be of interest to assess the potency of other divalent cations on hKv1.5 current. For example, external Ba^{2+} can interact with at least two distinct and sequential binding sites on the Shaker K^+ channel, resulting in a fast and a slow component of channel block (Hurst et al., 1996).

The authors express their thanks to Laurence Hilfiger for her expert assistance in the preparation of cultured cells.

References

Barry, D.M., Trimmer, J.S., Merlie, J.P., Nerbonne, J.M. 1995. Differential expression of voltage-gated K^+ channel subunits in adult rat heart. Relation to functional K^+ channels? *Circ. Res.* **77:**361–369

Delpon, E., Valenzuela, C., Gay, P., Franqueza, L., Snyders, D.J., Tamargo, J. 1997. Block of human cardiac Kv1.5 channels by loratadine: voltage-, time- and use-dependent block at concentrations above therapeutic levels. *Cardiovasc. Res.* **35:**341–350

Dumaine, R., Roy, M.L., Brown, A.M. 1998. Blockade of HERG and Kv1.5 by ketoconazole. *J. Pharmacol. Exp. Ther.* **286:**727–735

Fedida, D., Wible, B., Wang, Z., Fermini, B., Faust, F., Nattel, S., Brown, A.M. 1993. Identity of a novel delayed rectifier current from human heart with a cloned K^+ channel current. *Circulation* **73:**210–216

Feng, J., Wible, B., Li, G.R., Wang, Z., Nattel, S. 1997. Antisense oligodeoxynucleotides directed against Kv1.5 mRNA specifically inhibit ultrarapid delayed rectifier K^+ current in cultured adult human atrial myocytes. *Circ. Res.* **80:**572–579

Feng, J., Xu, D., Wang, Z., Nattel, S. 1998. Ultrarapid delayed rectifier current inactivation in human atrial myocytes: properties and consequences. *Am. J. Physiol.* **275:**H1717–H1725

Franqueza, L., Valenzuela, C., Delpon, E., Longobardo, M., Caballero, R., Tamargo, J. 1998. Effects of propafenone and 5-hydroxypropafenone on hKv1.5 channels. *Br. J. Pharmacol.* **125:**969–978

Hamill, O.P., Marty, A., Neher, E., Sakmann, B., Sigworth, F.J. 1981. Improved patch-clamp techniques for high-resolution current recording from cells and cell-free membrane patches. *Pflueg. Arch.* **391:**85–100

Hille, B. 1992. Ionic Channels of Excitable Membranes. Sinauer Associates Inc., Sunderland, MA. Second Edition

Ho, W.K., Kim, I., Lee, C.O., Youm, J.B., Lee, S.H., Earm, Y.E. 1999. Blockade of HERG channels expressed in *Xenopus laevis* oocytes by external divalent cations. *Biophys. J.* **76:**1959–1971

Hurst, R.S., Toro, L., Stefani, E. 1996. Molecular determinants of

external barium block in Shaker potassium channels. *FEBS Let.* **388:**59–65

Li, G.R., Feng, J., Yue, L., Carrier, M., Nattel, S. 1996. Evidence for two components of delayed rectifier K^+ current in human ventricular myocytes. *Circ. Res.* **78:**689–696

Longobardo, M., Delpon, E., Caballero, R., Tamargo, J., Valenzuela, C. 1998. Structural determinants of potency and stereoselective block of hKv1.5 channels induced by local anesthetics. *Mol. Pharmacol.* **54:**162–169

Malayev, A.A., Nelson, D.J., Philipson, L.H. 1995. Mechanism of clofilium block of the human Kv1.5 delayed rectifier potassium channel. *Mol. Pharmacol.* **47:**198–205

Mays, D.J., Foose, J.M., Philipson, L.H., Tamkun, M.M. 1995. Localization of the Kv1.5 K^+ channel protein in explanted cardiac tissue. *J. Clin. Invest.* **96:**282–292

Paquette, T., Clay, J.R., Ogbaghebriel, A., Shrier, A. 1998. Effects of divalent cations on the E-4031-sensitive repolarization current, I(Kr), in rabbit ventricular myocytes. *Biophys. J.* **74:**1278–1285

Philipson, L.H., Malayev. A., Kuznetsov, A., Chang, C., Nelson, D.J. 1993. Functional and biochemical characterization of the human potassium channel Kv1.5 with a transplanted carboxyl-terminal epitope in stable mammalian cell lines. *Biochim. Biophys. Acta* **1153:**111–121

Roberds, S.L., Knoth, K.M., Po, S., Blair, T.A., Bennett, P.B., Hartshorne, R.P., Snyders, D.J., Tamkun, M.M. 1993. Molecular biology of the voltage-gated potassium channels of the cardiovascular system. *J. Cardiovasc. Electrophys.* **4:**68–80

Shi, H., Wang, H.Z., Wang, Z. 2000. Extracellular Ba^{2+} blocks the cardiac transient outward K^+ current. *Amer. J. Physiol.* **278:**H295–H299

Song, D.K., Earm, Y.E., Ho, W.K. 1999. Blockade of the delayed rectifier K^+ currents, IKr, in rabbit sinoatrial node cells by external divalent cations. *Pflueg. Arch.* **438:**147–153

Tamkun, M.M., Knoth, K.M., Walbridge, J.A., Kroemer, H., Roden, D.M., Glover, D.M. 1991. Molecular cloning and characterization of two voltage-gated K^+ channel cDNAs from human ventricle. *FASEB J.* **5:**331–337

Wang, Z., Fermini, B., Nattel, S. 1993. Sustained depolarization-induced outward current in human atrial myocytes. Evidence for a novel delayed rectifier K^+ current similar to Kv1.5 cloned channel currents. *Circ. Res.* **73:**1061–1076

Yang, T., Prakash, C., Roden, D.M., Snyders, D.J. 1995. Mechanism of block of a human cardiac potassium channel by terfenadine racemate and enantiomers. *Br. J. Pharmacol.* **115:**267–274

Yu, S.P., Kerchner, G.A. 1998. Endogenous voltage-gated potassium channels in human embryonic kidney (HEK293) cells. *J. Neurosci. Res.* **52:**612–617

Zamponi, G.W., Bourinet, E., Snutch, T.P. 1996. Nickel block of a family of neuronal calcium channels: subtype- and subunit-dependent action at multiple sites. *J. Membrane Biol.* **151:**77–90